PROCEEDINGS, 46th Workshop on Geothermal Reservoir Engineering
Stanford University, Stanford, California, February 15-17, 2021
SGP-TR-218

Geology and Co-creation at Fly Ranch Hot Springs, Northwestern Nevada

Glenn Melosh

2685 Sunrise Ave, Santa Rosa, CA

gmelosh@gmail.com

Keywords: conceptual model

ABSTRACT

A conceptual model for Fly Ranch hot springs suggests that fractures held open near an active fault intersection provided the pathway for initial circulation of water deep into the thinning hot crust. Competing fault offsets jammed the intersection, locking movement, such that remnant extensional stresses, not released in fault offset, hold the cracks open to depth. Recent and glacial-age cold waters organized to flow down some of these open cracks and buoyantly rise in others in a single-pass circulation pattern. Circulating water gains heat at depth while cooling and shrinking the rock, causing further opening of deep fractures. Hot water dissolves limestone along fracture pathways as it rises, charging the water with calcium and carbonate ions. These ions subsequently re-deposit as travertine in spires at a cluster of hot water vents near the summit of a broad travertine mound about 1 km in diameter and 40 meters thick. The upflow feeds a shallow hot aquifer underlying the travertine mound and extending to the southwest (SW). Other hot aquifers may occur at greater depth.

Fractures held open by active stresses and deep-water circulation resulted in hydrothermal permeability feedbacks that support long-lived hot water flow to the surface. The consistent flow of heat and water in turn supports a vibrant and consistent living habitat. The surface springs and poolside evaporative zones are also open to cosmic fallout and solar energy. This combination of hot spring habitat and cosmic input may have nurtured the beginning of life in volcanic zones in the early earth.

Figure 1 – Fly Ranch Geyser by Patricia Melosh

1. INTRODUCTION

The travertine at Fly Ranch is riven by open fissures that align numerous hot springs and pools. The pools are surrounded by tall grasses while the hot water jetting from imposing travertine spires supports colorful thermophilic algae draping the spires in a beautiful centerpiece for the hot spring habitat (Figure 1).

Recognition of the inspirational beauty and utility of the hot water system at Fly Ranch and its location near the annual Burning Man festival in northwest (NW) Nevada led to purchase of the asset by the Burning Man Organization. Their intent to inspire broad input and cooperation in realizing creative, artistic, practical, and wise elaboration of the energy, water, and living resources at Fly Ranch led to this effort to provide a scientific context for how geologic processes support the surface condition. This report attempts to tell the story of the hot springs and identify connections between geologic and living processes to help inform the future of Fly Ranch.

The report starts by reviewing three foundational concepts followed by describing a geologic conceptual model for the Fly Ranch hydrothermal system. Then more detailed sections review aspects of the geologic model. Finally, hydrothermal process relationships are summarized in a holistic section that speculates on the combination of hydrothermal conditions and living processes in the springs.

2. FOUNDATIONS

2.1 **Extensional Faults and Fractures**

Features of extensional faults and associated secondary fractures allow deep water circulation that initiates hydrothermal system development in Nevada. There are three main types of these faults (Figure 2a). Fissures gape open due to movement on either side directly away from the fracture. Fissures occur in areas with low effective confining pressure (eg. near the surface or in zones of high fluid pressure) and can occur near the surface of other extensional faults. Normal faults show relative offset by movement of rock on the upper side of inclined fault plane, down the dip of the fault. Normal faults and fissures form perpendicular to the prevailing orientation of crustal extension in map view. Oblique-normal faults allow movement that is partly down the fault and partly lateral, along the fault. In some cases, oblique faults were originally formed as normal faults under a previous of orientation of extension and are still active although the offset direction has changed.

Fault movements cause secondary fractures in a zone around the primary offset surface, especially near fault irregularities. Secondary fractures can be the primary focus of permeability since offset can polish the main fault surface and fill it with ground-up fragments.

When many normal faults are expressed across broad extensional regions, they can help thin the crust of the earth. In some cases, large normal faults curve to be less steep at depth such that the normal fault blocks rotate as they slip (Figure 2b). In addition to the net thinning of the brittle zone, ductile rock at depth can neck down due to extension, such that hot mantle rock rises, promoting high heat flow.

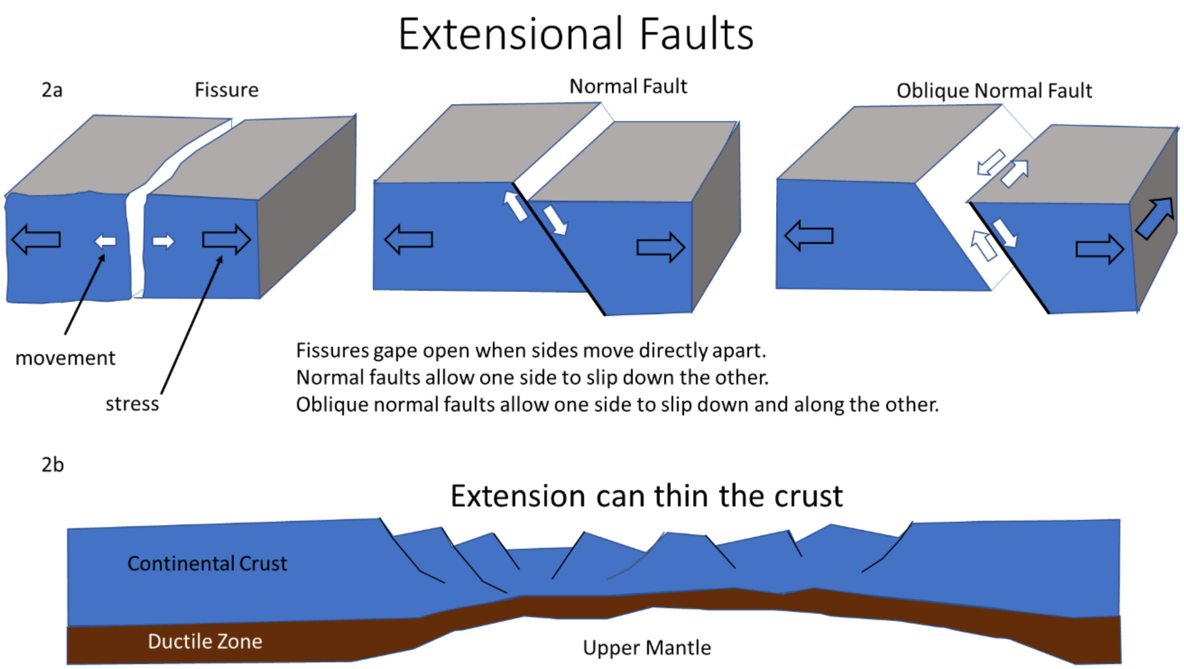

Figure 2 –Extensional Faults. 2a shows three types of extensional faults. 2b shows a simplified cross-section of extended crust.

2.2 **Fault Irregularities and Hydrothermal Permeability**

Comprehensive studies of the structural setting of more than a thousand hot springs in the Basin and Range Province and worldwide have demonstrated that roughly 95% of hot springs occur in areas with active locked structural irregularities, areas where irregular fault patterns such as fault bends and intersections do not allow complete relaxation of active tectonic stress through fault offset (Curewitz and Karson, 2008 and Faulds et. al., 2011). Remnant stresses focused at a locked irregularity include compressive and extensional concentrations. Extensional stress concentrations can hold open fractures to allow water circulation to depth while compressional concentrations on the other hand are often sealed. This hypothesis for the initial development of permeability in deep hydrothermal systems is based on hot spring distributions but is consistent with geothermal well results in various fields indicating that fracture opening continues beyond typical well depths of around 2 km depth. The hypothesis was tested by the successful targeting of a geothermal well at Blue Mt, about 100 km ENE of Fly Ranch (Melosh, 2008) based on a structural model by Faulds (Faulds and Melosh, 2008) and was formulated as a well-targeting method by Melosh (2016). Fault complexity in large geothermal fields can make the interpretation of remnant stress distributions difficult to interpret.

2.3 **Co-Creation**

Positive feedback is the primary mechanism that drives change in the natural world. Positive feedback refers to processes where an energy source drives change that then triggers more of the same change. This change accelerates as long as energy is available and it is not otherwise constrained. Systems with high energy throughput in multiple interacting feedback loops also self-organize and, in the process, create new patterns and characteristics, not inherited from their surroundings or physical condition. An oft-cited simple example is how convection cells get established in a heated pot of water. These self-organized systems can become stable due to the occurrence of co-operating negative feedback (where further change is limited by feedback) such that the new characteristics or, more broadly, personalities, can persist while energy and materials continue to flow through the system. The co-operation of multiple energy sources and feedback processes to create new patterns in a self-organized system is referred to here as co-creation. Hydrothermal systems are a moderately complex example (Melosh, 2019). (More information on self-organization is available from Heylighen, 2020).

3. FLY RANCH CONCEPTUAL MODEL

The anomalous heat in deep rock and the resulting hot spring expression in northwest Nevada are related to thinning of the crust of the earth (Heimgartner et. al., 2006). Thinning in the region is caused by active, roughly west-northwest (WNW), regional crustal extension that creates Basin and Range topographic patterns from widespread extensional normal faulting (Figure 3). Crustal thinning brings hot upper mantle rock closer to the surface while also supporting deep open cracks that allow water to access deep heat.

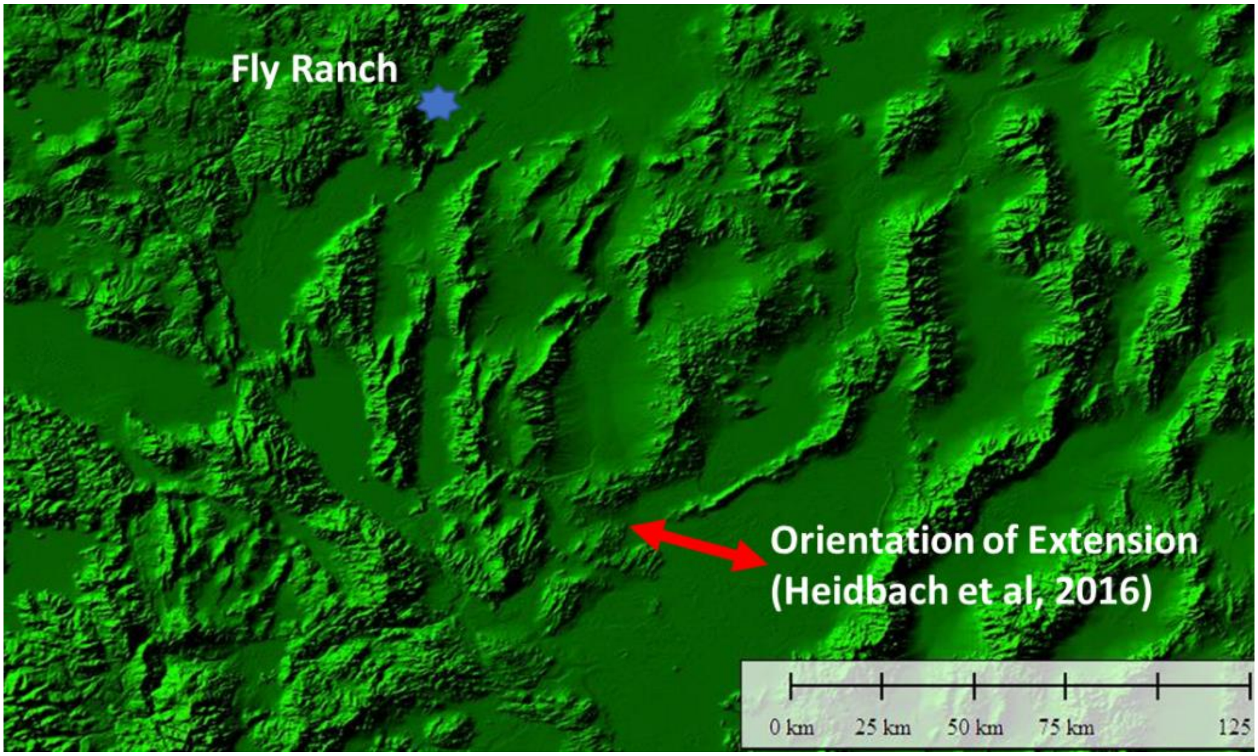

Figure 3 - Ranges and basins in NW Nevada are generally perpendicular to extension due to normal faulting.

Deep water circulation at Fly Ranch occurs along fissures and deeper fractures held open by stresses concentrated around a locked intersection between two active extensional faults at the travertine mound (Figure 4). The intersecting faults include a north-northeast (NNE) trending normal fault mapped along the west side of the Hualapai Flat, passing on the east edge of the travertine, and an older northeast (NE) trending oblique-normal fault interpreted south of the travertine. The open fractures just west of the intersection prominently include fissures that align hot springs in the travertine.

Granite Range runoff and cold groundwater descend on open fractures near the intersection to 2 to 2.5 km depth and then ascend on other fractures to the travertine mound. At depth the water is heated by hot granite to about 170°C after the water passes the deepest zone and then cools along the flow path to finally surface at 97°C. Cooling of water during the ascent through limestone allows dissolution of carbonate materials on the fractures. The dissolved carbonates later deposit at the surface as travertine.

Hot water storage occurs along this flow path in corroded limestone, pores and fractures in volcanic ash deposits, and in sandy gravel zones in the near surface basin sediments. Lake sediments and travertine partially cap the hot aquifers although they allow leakage on active fissures. Flow occurs in a single-pass from cold water source to hot spring outflow, not re-circulating in a convection cell.

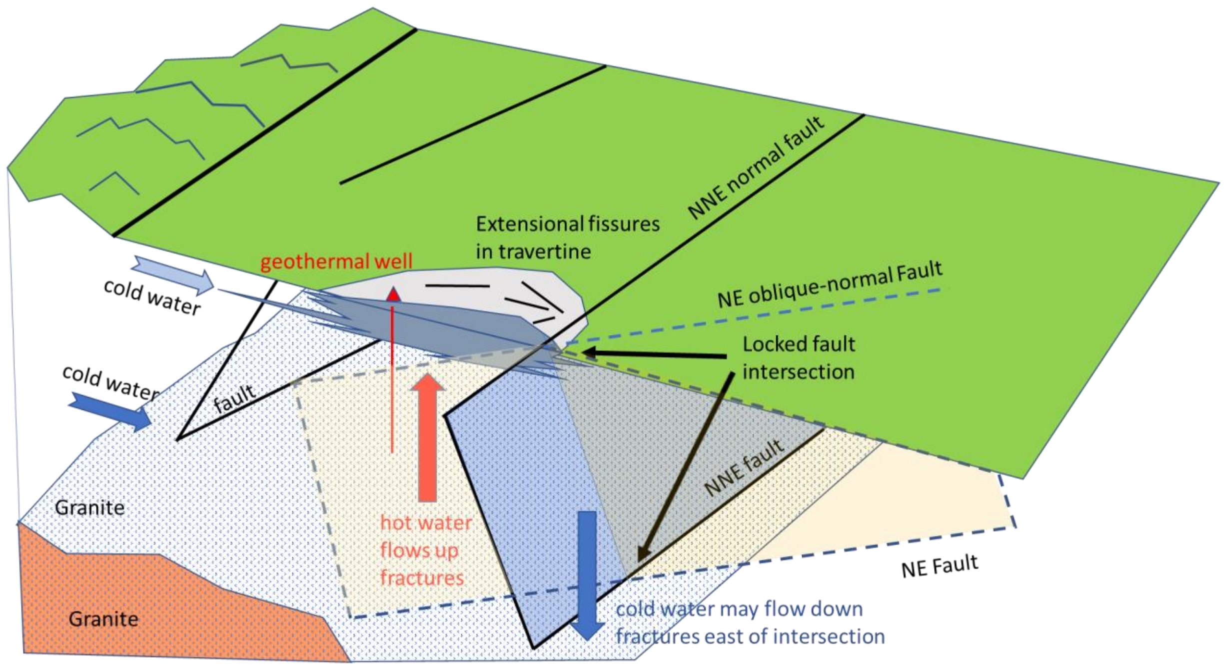

Figure 4 – Perspective View of Fly Ranch Conceptual Model. The model interprets a fault intersection shown by two inclined planes that extend below the surface and extend south of the cutaway (transparent orange and blue). The red arrow shows hot water upflow in open fissures west of the fault intersection. The blue down arrow shows a possible cold water downflow. Shallow cold water in gravel (light blue arrow) is sealed off from the hot spring circulation to at least 100 m depth. Deep cold water may also contribute to upflow. Granite (dotted) represents the deep conductive heat source.

4. ASPECTS OF THE CONCEPTUAL MODEL

4.1 Geology

Surface rock at the hot springs is composed of travertine. The travertine is surrounded and underlain by basin sediments. At greater depth these rocks are underlain by volcanic rocks, metamorphic rock, and granite successively. The surficial distribution of rocks in the region is shown in the geologic map (Figure 5). The pattern of these rocks at depth across the Hualapai Flat is interpreted in a cross-section (Figure 6).

Travertine is a rock composed of the minerals calcite and aragonite (forms of $CaCO_3$). Travertine forms due to CO_2 gas emission from carbonate-rich water at the surface as described in the geochemistry section below. The travertine at Fly Ranch covers more than 1 sq. km and rises above surrounding sediments by about 8 meters (Figure 7). Older portions of the travertine are probably buried in sediments such that the true thickness is greater. Local seismic reflection lines identify strong reflectors that might be due to travertine under the mound down to depths of 40 meters (Kratt, 2020). A travertine thickness of 40 meters would suggest a long duration of hot spring flow.

The travertine is underlain and surrounded by basin sediments. Local water well information shows that the basin sediments vary between permeable and porous gravels and sands and impermeable clay-rich lake sediments (Sinclair, 1962). These beds were laid down during the recent history of eroded sands and gravels shedding from the nearby mountains competing with lake sediment deposition associated with a large glacier-age lake. Recent playa sediments due to seasonal lake formation are widespread at the surface SE of Fly Ranch.

The sediments are underlain by Tertiary volcanic rock, including lava flows underlain by volcanic ash deposits (Grose and Sperandio, 1973). These rocks are widespread in the ranges north of the springs (Figure 5). Volcanic rocks can provide useful availability and storage of water since the lavas are strong enough to easily maintain open fractures and ash deposits can have high porosity and significant aquifer volume. The rock strength contrast at the boundaries of the lava flows may also lead to abundant local secondary fractures near fault irregularities. The volcanism is too old to represent a heat source for the hot springs.

Below the volcanic rock, metamorphic rock and underlying granite are thought to extend from where they outcrop in the Granite Range west of Fly Ranch and on Steamboat Ridge to the east. These crystalline rocks embody the heat source, fed by conductive heat flow from the upper mantle. The metamorphic rocks include limestones that outcrop in the Granite Range (Grose and Sperandio, 1973).

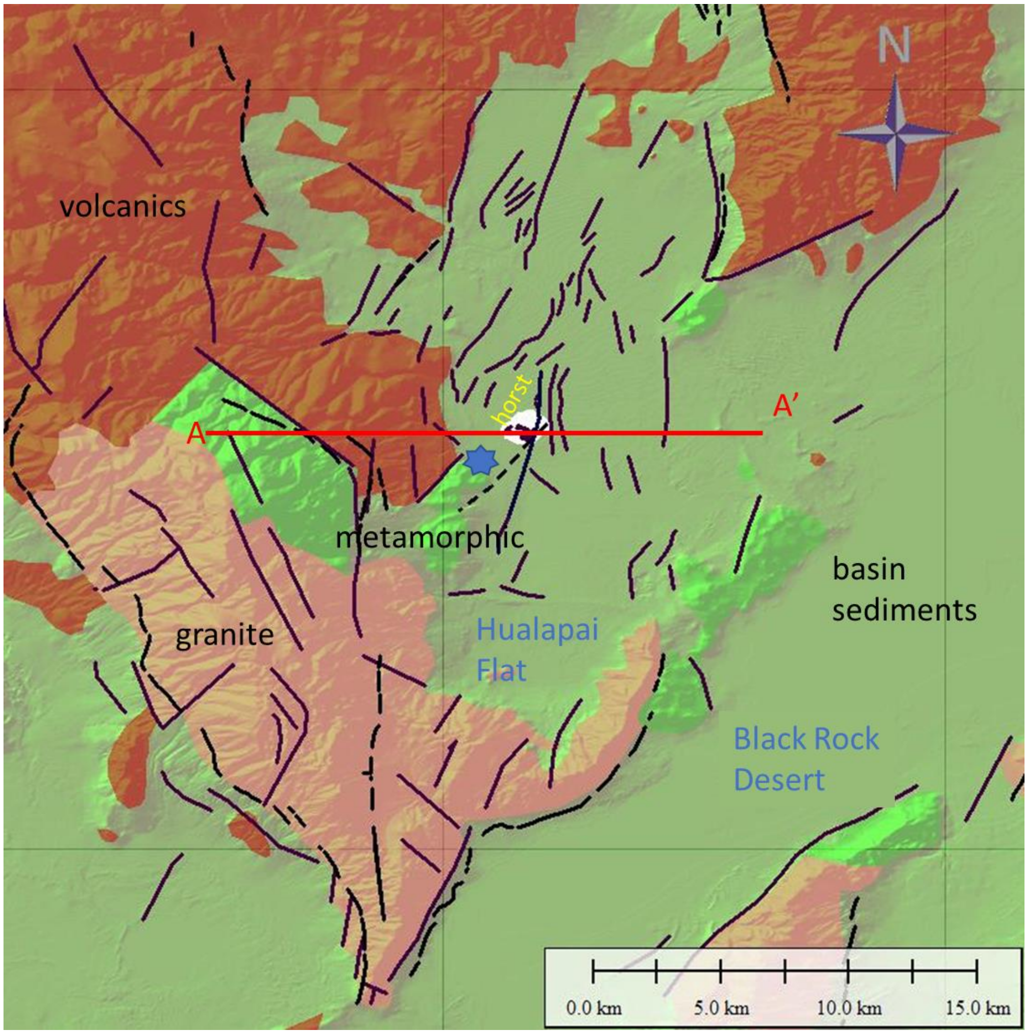

Figure 5 - Simplified Geology of Hualapai Flat and Surroundings. The rock distribution from south to north proceeds from granite, to metamorphic rock, to volcanics, surrounded by basin sediments. The travertine is white. Faults are shown by black lines. A buried horst is labeled in yellow. Geology is simplified from Grose and Sperandio (1973) and Schaefer et al (1981) and slightly adjusted to fit the more recently available detailed topography. A cross-section was drawn along the red line from A to A' (see Figure 6).

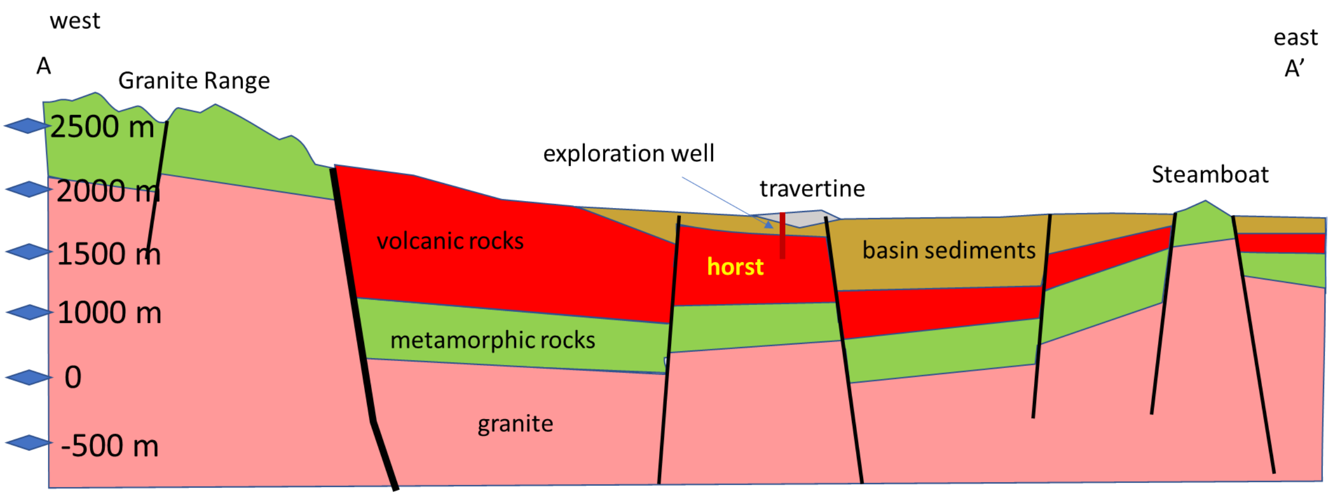

Figure 6 - Schematic Geologic Cross-Section Across Hualapai Flat at Fly Ranch (modified from Grose and Sperandio, 1973).

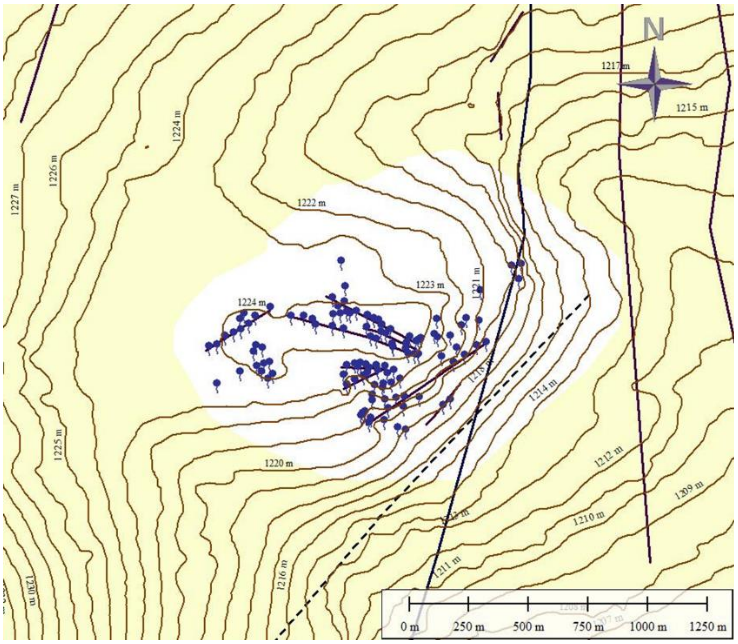

Figure 7 – Travertine Topography. 1-meter contours show a flat-top travertine mound (in white) with relatively steep sides. The tallest part of the mound is about 8 meters above local sediments as measured along the trend of basin topographic contours. The flat top of the mound has prominent fissure lineaments and hot springs shown by black lines and blue spring symbols. Black and dashed lines are faults. Spring locations are from Grose and Keller (1975).

4.2 Geologic Structure

Fault patterns observed in Hualapai Flat suggest that two active intersecting extensional faults may cause open fractures at the Fly Ranch Hot Springs.

The regional fault pattern around the Hualapai Flat includes several long normal faults with trends ranging from NW to NE. Repeated extensional offset on these faults has created the range-basin topography of the region including the Granite Range, Hualapai Flat, Calico Range, Steamboat Ridge, and the main Black Rock Desert basin. Current regional extension occurs in a west-northwest (WNW) orientation (Heidbach et. al., 2016) consistent with widespread NNE-trending fault block ranges (Figure 3).

Grose and Sperandio (Figures 5 and 6) show the distribution of faults in the Hualapai Flat based on detailed mapping. Near Fly Ranch faults crossing the Flat delineate an upthrown block (or horst) with normal faults on both sides that trends NNE from the area of the Fly Ranch travertine. The horst also shows up in the regional Depth to Basement map (Figure 8). Depth to Basement is calculated from gravity measurements and models for the density of basin sediments in contrast to the density of basement rock (ie granite, metamorphic, and volcanic rocks).

The Near Surface Temperature map (Figure 9) is another regional dataset that provides information on structure. This map is based on 223 temperature measurements made at 1-meter depth across Hualapai Flat and part of the Black Rock Desert (Keller et al, 1978). Temperatures were corrected for a variety of effects to better represent heat flow from the earth. Temperature measurement locations were not reported. Temperatures can be affected by the rock type (e.g. insulating or conductive) or shallow water flow among other influences. High values may be due to a more conductive rock in the near surface or hot water flow.

A NE-trending oblique-normal fault is interpreted just south of the hot spring area partly based on Near Surface Temperature. The interpretation includes NE-trending scarps on the south side of the travertine and in the Granite Range foothills nearby to the SW, the southern limit of the hot spring distribution, and the strong NE trend of the elongate shallow temperature anomaly (Figure 10). Grose (1973) suggested a fault in this location is an extension from a fault mapped at the southern tip of the Calico Range (Figure 5). Confirmation of whether the NE interpreted fault represents an observed fault should be sought by mapping the proposed fault line into the foothills.

An intersection between the NNE fault on the east edge of the horst block and the interpreted NE oblique-normal fault occurs just east of the hot springs (Figure 10). Movement on either of the intersecting faults would offset the other fault. The resulting fault discontinuity could lock the intersection causing remnant stress concentrations nearby. A structural diagram in Figure 11 interprets components of remnant compressive and extensional stresses near this fault intersection due to a proposed left-lateral offset on the NE fault. The actual stress distribution may be affected by unresolved stresses from both faults and is likely to be more complex. A pattern of open fissures evident from hot spring alignments supports the interpretation of an extensional stress concentration in the travertine.

The open fissure spring lineaments at Fly Ranch (Figure 12) appear very similar to spring and pool fissures in other spring deposit terraces, such as at the silica sinter terrace at Puchildiza, Chile. At Puchildiza there are hundreds of open (in many cases gaping), very well-exposed fissures, many with boiling hot water visible a couple meters down. The fissures in the Puchildiza sinter also occur in an extensional quadrant of a mapped fault intersection, like at Fly Ranch. Aligned hot springs are common in other areas as well.

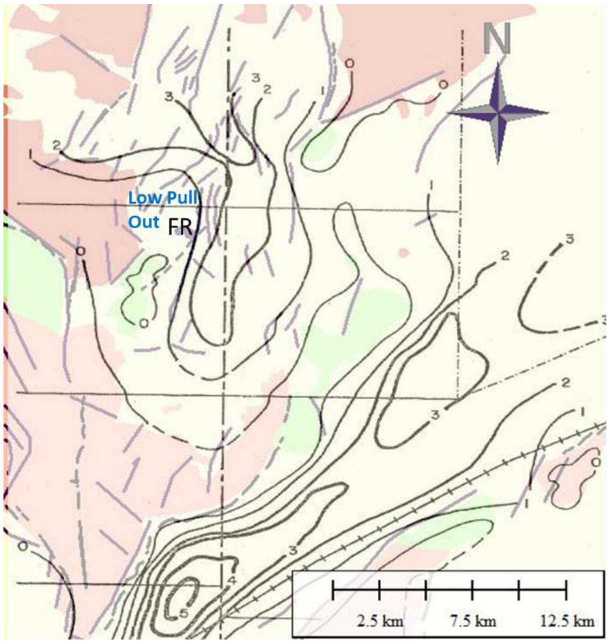

Figure 8 – Depth to Basement Map. Black contours show the depth from the surface to the bottom of the basin sediments across Hualapai Flat and Black Rock Desert in thousands of feet. These depths were based on gravity modeling (Keller et al, 1978). The low pull out (labeled in blue) marks a relatively low depth to basement indicating that basin sediments are relatively thin over the horst block at Fly Ranch (FR).

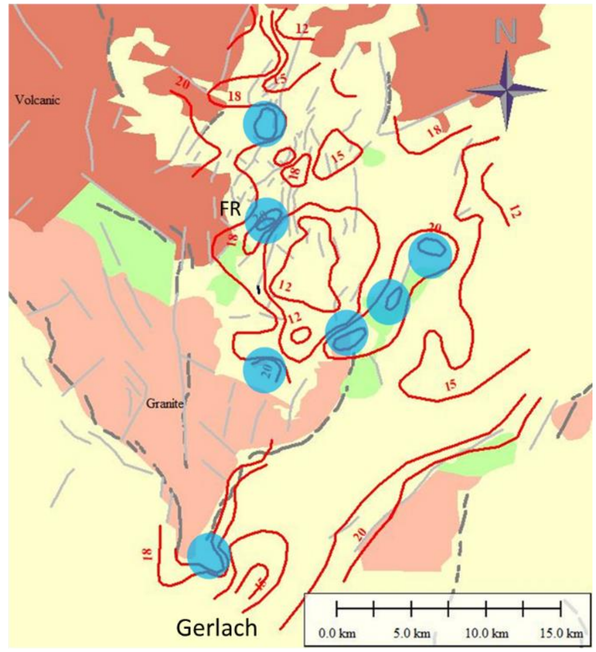

Figure 9 – Regional Soil Temperature Map. Contours show 1-meter depth temperatures at 12, 15, 18, and 20°C. Basins are cooler than ranges due to more insulating rock. 7 high temperature anomalies on the map are shown in blue. The 3 anomalies along the Steamboat Ridge may be due to higher conductivity rock. The 4 anomalies from Gerlach north through Fly Ranch (FR) suggest shallow warm water flow.

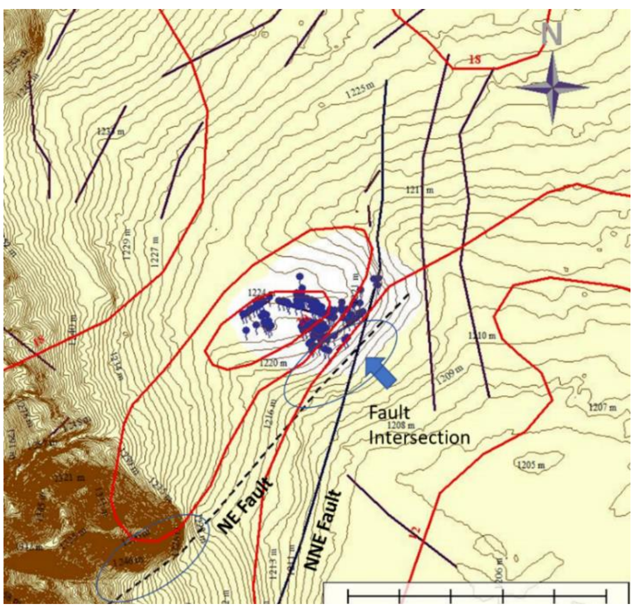

Figure 10 – Interpreted NE Fault at Fly Ranch. The dashed NE line interprets a fault that intersects with a solid line NNE fault mapped by Grose and Sperandio (1973). The dashed fault is based on topographic scarps at the range front and south of the springs (blue ovals) and soil temperature contours that show an NE trending elongate high (>18°C) extending SW of the travertine. This fault could act to stop hot water flow to the SE. Grose (1973) originally suggested a NE fault in this area that extends across the Flat to the Calico Range.

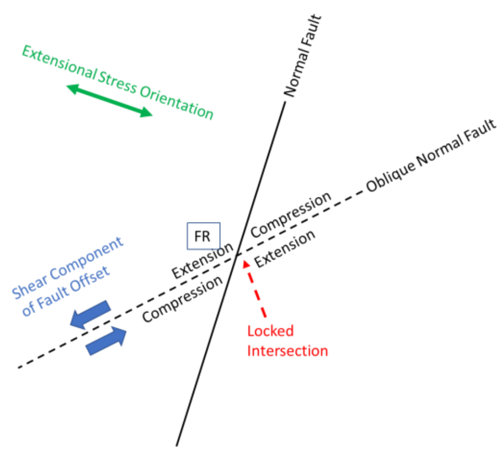

Figure 11 – Simple Example of Stress Near a Locked Fault Intersection. This example was drawn to be similar to the fault pattern at Fly Ranch but was simplified by only showing a map view and offset on one fault. Movement on the NE fault under current extension direction would be oblique left-lateral-normal offset (i.e. the other side of the fault moves to the left as well as vertically). Lateral offset on the NE fault would result in remnant stress accumulation around the intersection as labeled. Stress concentrations alternate around the intersection between extension and compression depending on whether the rock is pulled away or pushed at the locked intersection by block movement. In this example the Fly Ranch Hot Springs (FR) occur where remnant extensional stresses may be available to hold open fractures.

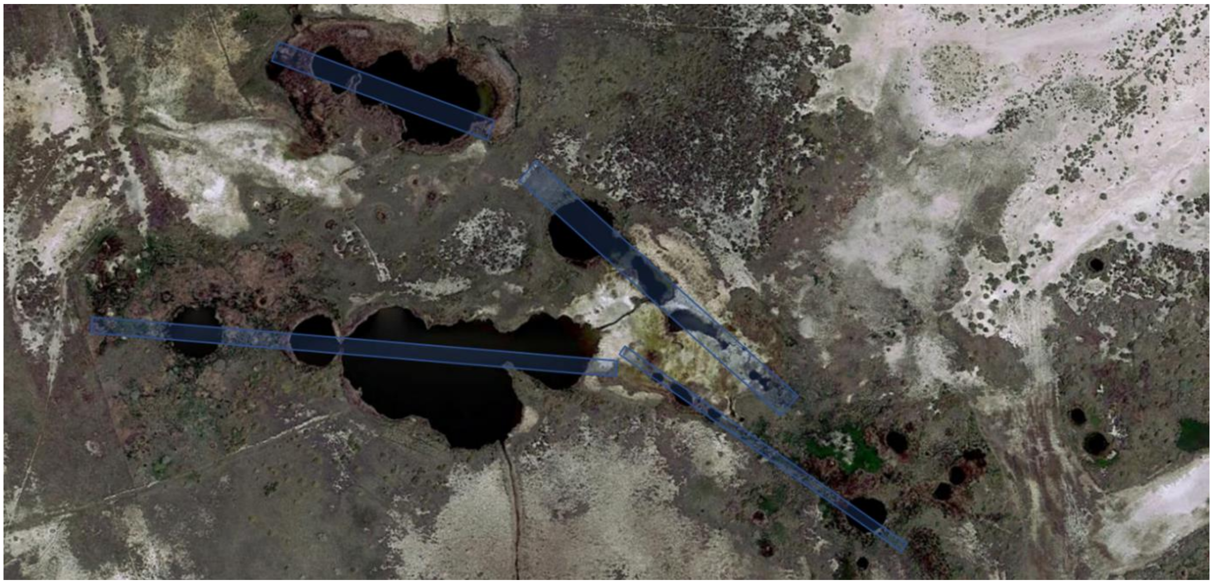

Figure 12 – Example spring and pool alignments reveal fissures in the Fly Ranch travertine. Blue bands show four of the fissures.

4.3 Fluid Geochemistry

Anderson (1973) reports 120 hot springs and 4 wells at Fly Ranch. Hot water produced by the springs and wells is relatively dilute at around 1000 ppm (parts per million) of total dissolved solids. The dissolved solids include all three common groundwater anions: bicarbonate, chloride, and sulfate, as well as the cations: sodium, potassium, calcium, and magnesium, along with silica. This pattern is typical of many hot spring systems worldwide. The dilute water chemistry does not show any indication of highly saline evaporite deposits in contact with water circulation in spite of the playa lake sediments deposited from water evaporation nearby to the southeast, probably due to a clay bottom seal in the lake bed.

The chemical data were compiled by the Great Basin Geothermal Center at the University of Nevada, Reno from various studies (NBMG, 2020a). The data were processed using the geothermal spreadsheet written by Powell and Cumming (2012). After filtering out problem data, the figures show that the remaining data show up as tight clouds in the plots (Figures 13 A to C).

Cation (positively charged ion) water composition shows evidence of thermal equilibration with minerals at various depths revealing a history of water temperatures that ranged up to as high as 170°C at depth, equilibrating in a shallower zone at 145°C and again at about 130°C before rising to measured surface temperatures of 97°C. This history is interpreted from geothermometers based on a combination of sodium and potassium (Na-K), then with calcium (Na-K-Ca), followed by equilibration between potassium and magnesium (K-Mg) and silica (as quartz) together, respectively, augmented by temperature measurement at the surface. Three figures are shown to reveal some of this history (Figure 13). These figures plot the compositions of the water samples and have lines showing typical geothermal equilibrium patterns. The Na-K geothermometer commonly indicates temperatures higher than measured in deep wells. It is controversial whether this indicates high temperature equilibration at depth below the wells or whether the minerals involved in equilibration chemistry differ from geothermometer assumptions. The surface temperature of the water is constrained by boiling, so the immediate near surface (pre-boiled) water temperature is probably higher than 97°C.

The anion (negative ion) chemistry of the spring water shows more bicarbonate but roughly equivalent concentrations of bicarbonate, chloride, and sulfate anions, all three of the common water anion species. These anions are dissolved out of the rock along circulation pathways. Typically, re-circulating geothermal systems include processes that result in deposition of calcite and anhydrite as water recycles through the system. This deposition strips bicarbonate and sulfate from source water, leaving dominantly chloride water that ends up slightly reduced and acidic. These conditions allow generation of hydrogen sulfide gas, (H_2S). Gases have not been sampled at Fly Ranch but the lack of H_2S odor is a strong indication that it is absent. The deviation of Fly Ranch waters from the chemical condition of re-circulating systems suggests that Fly Ranch circulation may follow a single-pass flow through the system and does not re-circulate.

The calcite and aragonite mineral deposition that forms the travertine spires and terraces at Fly Ranch is caused by gas separation during and after boiling as the water exits the circulation pattern. Even though full fluid chemistry and biochemical processes are more complex, calcite deposition can be described by a fairly simple reaction where water, CO_2, and calcite react with calcium and carbonate ions:

$$H_2O + CO_2 + CaCO_3 \leftrightarrow Ca^{++} + 2\ HCO_3^{-}$$

($CaCO_3$ is calcite or aragonite mineral and Ca and HCO_3 (bicarbonate) are dissolved ions. "↔" indicates the reaction will go either way.)

This expression refers to a chemical balance between components on the two sides of the reaction. Addition or removal of components on either side will result in reactions that proceed to rebalance chemical ratios between the components.

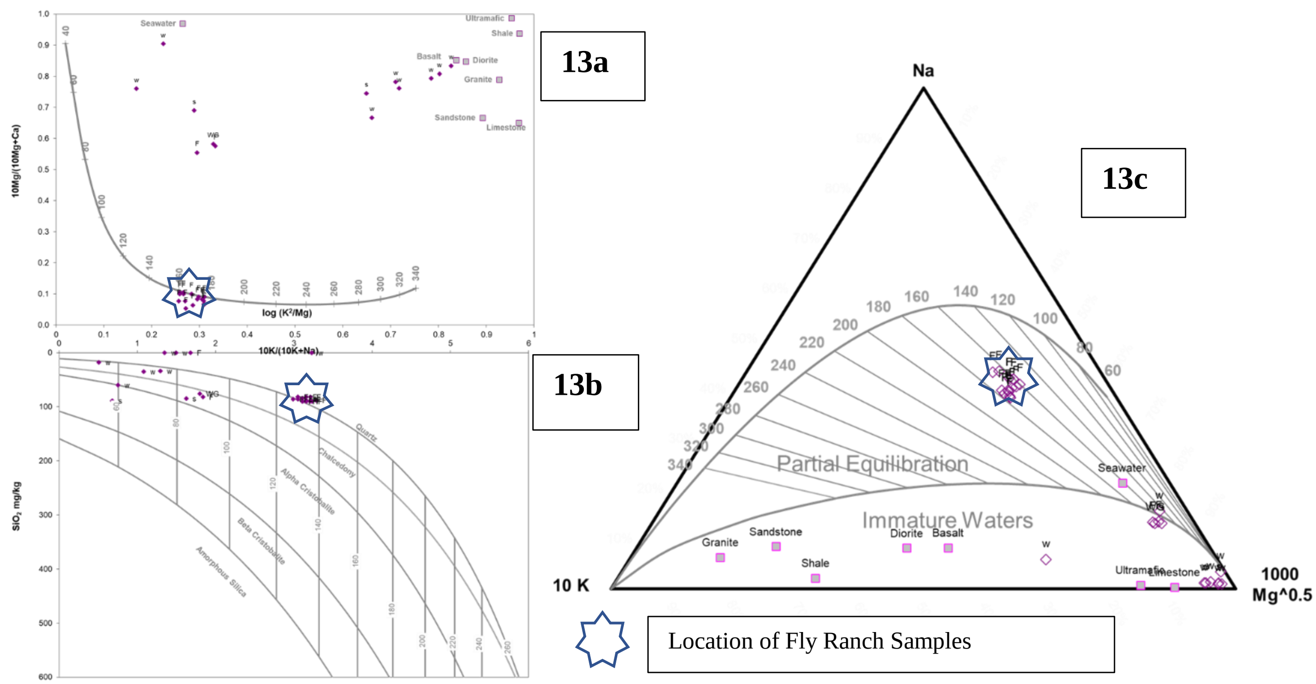

Figure 13 – A - Plot between a combination of potassium (K) and sodium (Na) concentrations vs. a combination of magnesium (Mg) and calcium (Ca) concentrations. The curved line shows the distribution at equilibrium with typical geothermal minerals at various temperatures. The Fly Ranch analyses show equilibrium at 170°C. Other cold springs and wells show different chemistry. B- Plot between silica (SiO_2) concentration and potassium-magnesium (K^2/Mg) geothermometry. The curved lines show the equilibrium patterns with different crystal forms of silica. Fly Ranch springs show equilibrium between the quartz and K^2/Mg at about 130°C. Quartz equilibration is typical of high temperature systems. C - Diagram showing thermal equilibration patterns for sodium (Na), potassium (K), and magnesium (Mg). The upper curve shows high temperature equilibration. The lines radiating to the Mg corner represent the increase in Mg as the fluid rapidly re-equilibrates to lower temperature while the much more stable Na-K ratio remains unchanged. The Fly Ranch springs (F) apparently equilibrated at 170°C (Na-K) and then re-equilibrated to lower temperature.

When the hot water boils in the vents, a little H_2O and nearly all of the CO_2 separate as gases and blow off. To re-acquire the chemical balance, the reaction will proceed to the left to re-generate dissolved CO_2 such that $CaCO_3$ also forms. The drastic drop of dissolved CO_2 during boiling drives very rapid deposition of calcite that forms the travertine spires, even restricting the spire vent openings to form jets.

As the water cascades off the spires and across the terraces after boiling, some areas in the flow of the water will have slightly lower pressure than other parts of the flow. Local sites of low pressure can be due to flow acceleration, such as where the water flows over the edge of a terrace. This causes minor degassing of (re-generated) CO_2 and deposition of travertine at the terrace lip. In other areas algal mats, organic detritus, or just other travertine can also nucleate deposition. Deposition can occur along the flow as long as Ca and HCO_3 ions are abundant in the water. Travertine terraces are also common around carbonate-rich cold-water springs due to the same process.

The large volume travertine mound at Fly Ranch is clearly anomalous relative to other local hot springs and requires a persistent source of carbonate ions (Ca^{++} and HCO_3^-) along the circulation path. This could be due to limestone (a carbonate rock) occurring at depth (Grose and Sperandio, 1973), consistent with outcrop evidence for limestone in the metamorphic rock formation in the area. Dissolution of the limestone into the water is most likely to occur along the flow path where fluid temperatures are decreasing. Carbonate solubility in water increases as temperature decreases so the fluid will scavenge carbonate from the limestone as temperature declines. Consequently, the limestone probably occurs in the upflow part of the circulation path directly below Fly Ranch.

4.4 Western Geothermal Well

In 1964 Western Geothermal drilled an exploration well at Fly Ranch. Very limited well records indicate that the well was drilled to 302 m depth and produced 440 gpm (gallons per minute) at a measured temperature of 97°C during a well test (NBMG, 2020b). This very high flow rate indicates that the water flowed into the well along open fractures. The depth of the entry of fluid into the well was not reported. The temperature measurement may have been made at the rig flow line after boiling so it is not necessarily representative of downhole water temperature.

This well has been leaking at a low rate for many years. Although the leaking well at Fly Ranch is commonly referred to as a "geyser", the well technically produces artesian flow of boiling water. The strict definition of a geyser specifies natural episodic or temporary flow.

During the episodic flow of a geyser, boiling proceeds downward until the immediate water supply is exhausted, after which the geyser goes through a recovery period. At Fly Ranch the flow is consistent, in an artificial structure, and boiling remains at the surface.

The artesian flowing pressure is probably related to the relatively low density of hot water. In a U-tube balance model, a column of dense cold water will lift a taller column of light hot water. Based on likely average temperatures and salinities of connected hot and cold-water columns at Fly Ranch and an estimated artesian lift height at the flowing well, a depth to the connection between cold and hot water columns can be calculated. This model suggests a hydrologic connection between hot and cold waters at a depth below 100 to 200 m. Shallower connections between the hot and local cold waters may be sealed by minerals, clay, or fault-offsets.

There are two main pathways for leakage from geothermal wells, either up the wellbore inside the casing and through a leak in the valve or well abandonment cement, or up the annulus between the steel casing and rock. These can occur together or at different depths in the same well and might connect at a casing break. Observations of the flowing well temperature at the Fly Ranch well after a rainstorm show that cold rainwater dampens the temperature of flow for about 2 weeks (Anderson, 1973). Consequently, it appears that the leak is probably coming up the annulus, at least near the surface, where it mixes with rain water. This type of leak is very difficult to fix. The leak through the annulus must be above a deeper zone where the hot water is isolated from cold groundwater to produce the long-term artesian flow. Oddly, the consequences of the leakage, i.e. the travertine spires, are one of the most valuable aspects of Fly Ranch, so although a leaking well would normally be an owner liability, at Fly Ranch it is the focus of value.

4.5 Hydrology

Water circulation in fractures at Fly Ranch may penetrate as deep as 2.5 km. This maximum depth estimate is based on the maximum estimated water temperature from Na-K geothermometry and the regional temperature gradient (pattern of temperature vs. depth) estimated from measurements in low gradient shallow wells in the Black Rock Desert (Figure 14).

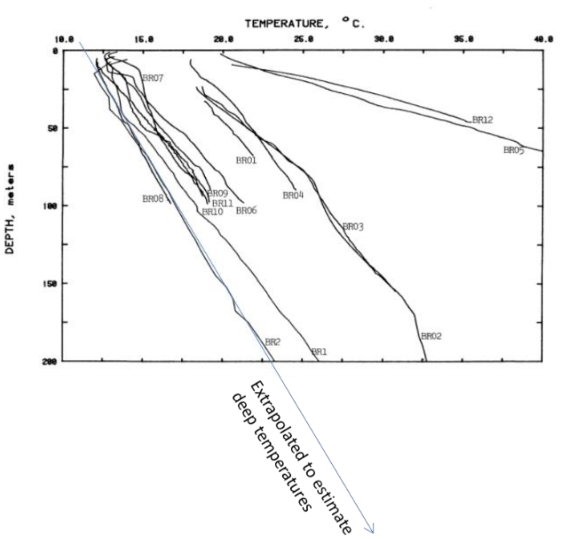

Figure 14 – Estimated Depth to 170°C. The plot shows temperature versus depth for wells drilled in the Black Rock Desert-Hualapai Flat area (Mase and Sass, 1980). The lowest gradient temperature profile (to the left) was used to extrapolate to deep temperatures in crystalline rock because higher gradient wells are probably affected by rising hot water or insulating (higher gradient) basin sediments. The gradient applied was 65°C/km which is about twice the global average and is appropriate for the region. The estimated depth to 170°C based on this plot is about 2.5 km. Both the gradient and highest fluid temperature are uncertain so the depth estimate is approximate.

The downflowing cold water source area is unknown but is probably along other fractures nearby, fed by groundwater and rainfall or runoff. This downflow might occur in the other extensional quadrant southeast of the intersection (Figure 10 and 5) as suggested by the much lower near surface temperatures in that area. Alternatively, deep ground water from aquifers fed by stream runoff or long-term storage in sediments may feed circulation.

As hot water rises out of the deep fractured granite, it encounters limestone and metamorphic rocks, porous volcanic ash and fractured lavas, basin sediments, and then a cap of impermeable lake sediments and travertine deposits. Along the way corroded limestone, porous volcanic ash, and gravel-rich sedimentary zones may store hot water.

Flow of hot water to the surface from an underlying aquifer occurs at several points across the travertine mound. These local upflows are revealed by a scattering of vents above 80°C surrounded by vents at much lower temperature, commonly below 40°C (Figure 15). Multiple scattered upflows suggest a broad shallow hot aquifer rather than an outflow tongue from a single narrow upflow.

Two other hot water upflows on the west side of Hualapai Flat are evident in near surface temperature measurements (Figure 9). One occurs to the south at Granite Springs and was the site of an exploration well that encountered a shallow well blow-out. More detail on the blow-out is not available. The other is to the north. The northern upflow is also evident in warm water flows in some water wells in the area (Sinclair, 1962). More upflow occurs farther south on the same north-trending fault line near Gerlach. All of these are probably related to separate fault irregularities and deep-water circulation pathways and are unlikely to be connected.

5. CO-CREATION

5.2 Hydrothermal Co-Creation

Most of this report summarizes detailed work on physical context of Fly Ranch geology, geophysics, and water chemistry observed by researchers from the Colorado School of Mines, the USGS, and the State of Nevada. However, the formation of a hydrothermal system is also strongly influenced by the interaction of a wide variety of hydrothermal processes that modify fractures and minerals in the rock. These processes include a network of positive and negative feedback loops that modify fracture permeability to enhance and reduce flows in different zones.

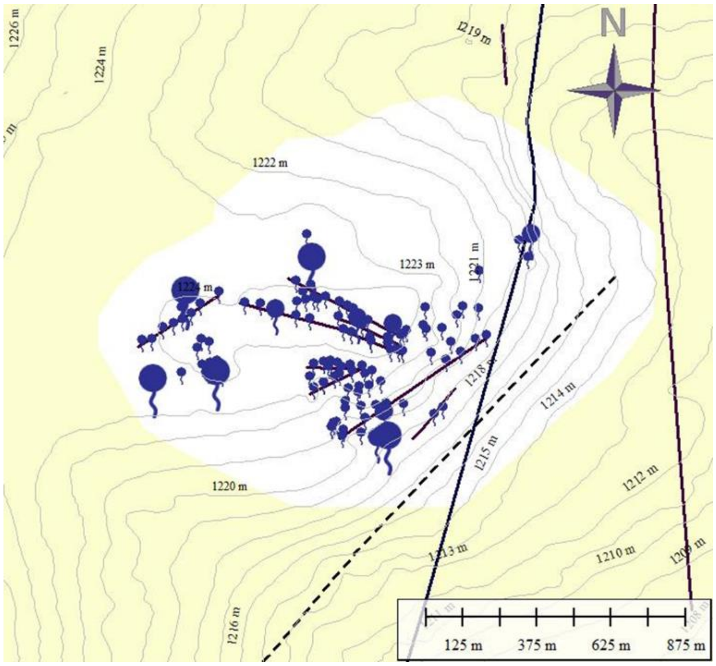

Figure 15 - Spring Temperature Distribution. Hot spring locations from Grose and Keller (1975) are shown by blue dots with wiggle tails. The largest symbols show springs over 80°C. The medium size symbols are 40 to 80°C. The small symbols are less than 40°C. The travertine is white. The distribution shows multiple high temperature vents scattered across the travertine immediately west of the fault intersection. Fissure alignments are based on multiple aligned springs and air photo lineaments.

Hydrothermal system formation can be initiated by earthquakes on active irregular faults that leave remnant extensional stresses to hold secondary fractures open. If the open fractures extend down to hot rock at depth and threshold convective water circulation begins, fracture permeability can be strongly increased by cooling (at depth) and decreased by heating (shallow) in several thermal-mechanical feedback processes (Melosh, 2019). For example, when heat transfers to the water at depth it locally cools and shrinks the rock. To accommodate rock shrinkage, the cracks in the rock open up further. Opened fractures then allow more rapid and widespread cooling, accelerating the processes of heat transfer, flow, and fracture opening.

The same fractures conduct water that promotes mineral dissolution, alteration, and deposition feedback processes that further modify permeability and can act to prop cracks open or seal them off in different zones. An example of negative feedback occurs where water boils as it flows up shallow cracks. The boiling fluid deposits minerals (like calcite) that act to seal cracks to limit flow.

Overall multiple feedback loops are driven by sources of mechanical, thermal, and chemical energy that drive co-creation of a self-organized system that creates fracture opening at depth and sealing near the surface. These complex interactions cooperate to focus available energy, complexity, and beauty that persists over the long term, much beyond fault movement periods.

At Fly Ranch the instigation for this co-creation comes from the open fractures associated with offset of an active horst block by a cross-fault as described above. Water stored in the basin and from rainfall circulates, triggers feedback, and delivers hot water to the surface. This process connects the Fly Ranch reservoir zones and acts to chemically seal the surface as evident in the large travertine deposit. Continued fault stress accumulation from tectonic forces then re-cracks the shallow seal to allow the deeper system to express itself at the surface again. Meanwhile at greater depths, mineral alteration and deposition decorate the rock with colorful minerals. At much later times these systems can be uplifted and then exhumed by erosion to show off their colors, like at the extinct hydrothermal system revealed in the Calico Range east of Fly Ranch.

5.2 Life

The earth opens itself to water circulation, that co-creates a hydrothermal system, that nurtures life and the co-creation of life at the surface in volcanic areas. Co-created hot spring systems on land support long term, warm, moist, moderately saline, habitat at the surface where life gathers to enjoy the water. Hot springs are also open to cosmic contributions ranging from dust to meteorites and solar energy in a setting with pulses of water flow that allow poolside evaporation events. These features have led to land-based volcanic hot springs becoming a leading hypothetical site for the creation of life on earth. The rationale for this hypothesis is described in detail by Damer and Deamer (2020). Their hypothesis simply put is that land-based hot springs with volcanic and cosmic input can include all the key components required for life including amino acids and lipids and provide the episodic dehydrating conditions essential to life formation at pool side sites. Even the bubbles associated with hot water gas emission might play a role if they help configure the lipid envelopes crucial to proto-cell development.

An alternative model for the beginning of life on earth suggests delivery of life material to earth in a meteorite, like the meteorites occasionally found on the playa of the Black Rock Desert. This alternative model suggests that life on earth was triggered by a meteorite landing in a hot spring. There is even a controversial meteorite sample (ALH84001) held at the Smithsonian interpreted to show signs of life (Choi, 2016). This meteorite was originally ejected from Mars by a much larger meteorite impact on that planet and then travelled across the solar system to land on earth. The meteorite with possible signs of life also shows evidence of hydrothermal alteration that occurred during its history on Mars (Treiman et. al., 2002). The likelihood of cosmic transport of life and life materials to earth from Mars has been assessed by Nicholson (in press).

These two alternatives both suggest that life may have begun in a hot spring, although we are not sure which planet it was on at the time. While these alternatives remain hypothetical, it is nevertheless clear from direct observation that co-creative hydrothermal systems support co-creative living systems in hot springs. At Fly Ranch our challenge is to accept this gift, whatever it means, and pay it forward.

6. REFERENCEES

Anderson, J.; 1973: A Geochemical Study of the Southwest Part of the Black Rock Desert and Its Geothermal Areas; Washoe, Pershing, and Humboldt Counties, Nevada

Choi, C.; 2016: Mars Life? 20 Years Later, Debate Over Meteorite Continues; Space.com, https://www.space.com/33690-allen-hills-mars-meteorite-alien-life-20-years.html

Crafford, A.; 2010: Geologic Terrane Map of Nevada; *Nevada Bureau of Mines and Geology Open File Report 10-4,* scale 1:500,000.

Curewitz, D. and J. Karson; 1997: Structural Settings of Hydrothermal Outflow: Fracture Permeability Maintained by Fault Propagation and Interaction; *Jour. of Volc. And Geothermal Research*, 79, pp. 149-168

Damer, B., D. Deamer; 2020: The Hot Spring Hypothesis for an Origin of Life; *Astrobiology*, Vol 20, No. 4; https:dpo.org/10.1089/ast2019.2045

Faulds, J., N. Hinz, M. Coolbaugh, P. Cashman, C. Kratt, G. Dering, J. Edwards, B. Mayhew, and H. McLachlan; 2011: Assessment of Favorable Structural Settings of Geothermal Systems in the Great Basin, Western USA; *GRC Transactions*, Vol 35, pp. 777-783

Faulds, J. and G. Melosh; 2008: A Preliminary Structural Model for the Blue Mountain Geothermal Field, Humboldt County, Nevada; *GRC Transactions*, Vol 32, pp. 273-278.

Grose, L. and G. Keller ed.; 1975: The Colorado School of Mines Nevada Geothermal Study, Progress Report No. 4; 112 pp.

Grose, L. and R. Sperandio; 1973: Geology of the Gerlach-Hualapai Flat Geothermal Area, Northwestern Nevada; *Colorado School of Mines Quarterly* 73-3; 10 pp.

Grose, L.; 1973: Late Quaternary Tectonic Controls of the Occurrence of Geothermal Systems in Gerlach-Hualapai Flat Area, Northwestern Nevada; *Colorado School of Mines Quarterly*, 73-3; 4 pp.

Heidbach, Oliver; Rajabi, Mojtaba; Reiter, Karsten; Ziegler, Moritz (2016): World Stress Map 2016. GFZ Data Services. https://doi.org/10.5880/WSM.2016.002

Heylighen, F.: The Science of Self-Organization and Adaptivity; http://pcp.vub.ac.be/Papers/EOLSS-Self-Organiz.pdf

Heimgartner, M., J. Louie, J. Scott, W. Thelen, C. Lopez, M. Coolbaugh; 2006: The crustal thickness of the Great Basin: Using seismic refraction to assess regional geothermal potential, *GRC Transactions*, 30

Keller, G., L. Grose, and R. Crewdson; 1978: Geophysical Exploration for Geothermal Prospects North of Gerlach, Nevada; Draft Report Colorado School of Mines; 74 pp.

Kratt, C.; 2020; Hualapai Flat and Fly Ranch Geophysical Report: University of Nevada, Reno preliminary report.

Kuamoto, L.; 1978: Microearthquake Survey in the Gerlach-Fly Ranch Area of Northwestern Nevada; *Colorado School of Mines Quarterly*, 73-3; pp. 45-64.

Mase, C. and J. Sass; 1980: Heat Flow from the Western Arm of the Black Rock Desert, Nevada; *USGS Open File Report* 80-1238.

Melosh, G. 2019: Release the Kraken – How Geothermal Feedback Forms Fractures; *Proceedings 44th Workshop on Geothermal Reservoir Engineering*, Stanford University

Melosh, G.; 2016: Geothermal Well Targeting Method Using Structural Irregularities; *Proceedings 40th Workshop on Geothermal Reservoir Engineering*, Stanford University, SGP-TR-204

Melosh, G.; 2008: Geothermal Drilling Success at Blue Mountain, Nevada; *Proceedings 33rd Workshop on Geothermal Reservoir Engineering*, Stanford University

NBMG, Nevada Bureau of Mines and Geology, 2020a: Great Basin Groundwater Geochemical Database; website: http://www.nbmg.unr.edu/Geothermal/GeochemDatabase.html

NBMG, Nevada Bureau of Mines and Geology, 2020b: Geothermal Well Information
http://www.nbmg.unr.edu/Geothermal/WellInfo.html

Nicholson, W.; in press: Ancient Micronauts: Interplanetary Transport of Microbes by Cosmic Impacts; *Trends in Microbiology*, doi:10.1016/j.tim.2009.03.004

Powell, T. and W. Cumming; 2012: Liquid Chemistry Plotting Spreadsheet; http://geothermaldata.org/content-model/powell-and-cumming-geothermometry

Schaefer, D., A. Welch, and D. Maurer; 1981: Geothermal Resources of the Western Arm of the Black Rock Desert, Part I, Geology and Geophysics; *USGS Open File Report* 81-918; 42 pp.

Sinclair, W.; 1962: Ground-Water Resources of Hualapai Flat; Washoe, Pershing, and Humboldt Counties, Nevada; *Ground-Water Resources - - Reconnaissance Series Report* 11, 16 pp.

Treiman, A., H. Amundsen, D. Blake, and T. Bunch; 2002: Hydrothermal Origin for Carbonate Globules in Martian Meteorite ALH84001: A Terrestrial Analogue from Spitsbergen (Norway); *Earth and Planetary Science Letters*, 204, pp 323 - 332